



Article

Engineering of multiferroic BiFeO₃ grain boundaries with head-to-head polarization configurations

Mingqiang Li^{a,b,c,1}, Shuzhen Yang^{d,e,i,1}, Ruochen Shi^{a,b}, Linglong Liⁱ, Ruixue Zhu^{a,b}, Xiaomei Li^f, Yang Cheng^{c,g}, Xiumei Ma^a, Jingmin Zhang^a, Kaihui Liu^{c,g}, Pu Yu^{h,i,*}, Peng Gao^{a,b,c,h,*}

^aElectron Microscopy Laboratory, School of Physics, Peking University, Beijing 100871, China

^bInternational Center for Quantum Materials, School of Physics, Peking University, Beijing 100871, China

^cAcademy for Advanced Interdisciplinary Studies, Peking University, Beijing 100871, China

^dPeking University Shenzhen Graduate School, Peking University, Shenzhen 518055, China

^eTCL China Star Optoelectronics Technology Co., Ltd., Shenzhen 518132, China

^fBeijing National Laboratory for Condensed Matter Physics and Institute of Physics, Chinese Academy of Sciences, Beijing 100190, China

^gState Key Laboratory for Mesoscopic Physics, School of Physics, Peking University, Beijing 100871, China

^hCollaborative Innovation Centre of Quantum Matter, Beijing 100871, China

ⁱState Key Laboratory of Low Dimensional Quantum Physics and Department of Physics, Tsinghua University, Beijing 100084, China

ARTICLE INFO

Article history:

Received 14 August 2020

Received in revised form 30 October 2020

Accepted 14 December 2020

Available online 29 December 2020

Keywords:

Head-to-head

Grain boundaries

Atomic structure

BiFeO₃

ABSTRACT

Confined low dimensional charges with high density such as two-dimensional electron gas (2DEG) at interfaces and charged domain walls in ferroelectrics show great potential to serve as functional elements in future nanoelectronics. However, stabilization and control of low dimensional charges is challenging, as they are usually subject to enormous depolarization fields. Here, we demonstrate a method to fabricate tunable charged interfaces with $\sim 77^\circ$, 86° and 94° head-to-head polarization configurations in multiferroic BiFeO₃ thin films by grain boundary engineering. The adjacent grains are cohesively bonded and the boundary is about 1 nm in width and devoid of any amorphous region. Remarkably, the polarization remains almost unchanged near the grain boundaries, indicating the polarization charges are well compensated, i.e., there should be two-dimensional charge gas confined at grain boundaries. Adjusting the tilt angle of the grain boundaries enables tuning the angle of polarization configurations from 71° to 109° , which in turn allows the control of charge density at the grain boundaries. This general and feasible method opens new doors for the application of charged interfaces in next generation nanoelectronics.

© 2020 Science China Press. Published by Elsevier B.V. and Science China Press. All rights reserved.

1. Introduction

Interfaces with high density of charges possess some intriguing properties such as insulator–metal transitions [1–3], superconductivity [4,5], magnetoelectric coupling [6–8] and photoconductivity [9,10], which enable charged interfaces to act as active elements in future nanoelectronics [11–13]. These charged interfaces usually occur as either heterointerfaces between different semiconductors and metal oxides [5,14–16] or homointerfaces in ferroic materials such as ferroelectric domain walls [1,17–22]. While heterointerfaces are fixed in space, homointerfaces like charged domain walls in ferroelectrics can serve as powerful tools to control the charged interface due to the switchability of the spontaneous ferroelectric

polarization. This phenomenon, which has attracted attention of researchers recently [1,17,20,21], is attributed to the polarization orientation-dependent screening charges at the interface that compensates the depolarization field [23–25]. The formation of a sheet of degenerate charged gas at the interface can exert dramatic changes in local electronic structure and evoke unusual physical properties over a range of several nanometers [26,27].

Unfortunately, charged domain walls with head-to-head or tail-to-tail polarization configurations are typically unstable due to incomplete screening of the bound charges that induce enormous depolarizing fields [26,27]. Nevertheless, there are sparse reports of charged domain walls, which suggest charged interfaces might be energetically favorable under some specific conditions [20,26]. For example, head-to-head and tail-to-tail charged domain walls have been observed in flux-closure domain pattern in BiFeO₃/GdScO₃ heterostructures [28]. A tetragonal-like crystal structure at the head-to-head charged domain wall can be locally stabilized at the surface and interface of BiFeO₃ thin films [24]. In addition,

* Corresponding authors.

E-mail addresses: yupu@mail.tsinghua.edu.cn (P. Yu), p-gao@pku.edu.cn (P. Gao).

¹ These authors contributed equally to this work.

charged domain walls are commonly observed during the ferroelectric switching process [29], although the very tiny size and intermediate nature make them impossible to be manipulated for practical purposes.

Here, we explore the controllability of stable charged interfaces in multiferroic BiFeO₃ thin films by grain boundary engineering. SrTiO₃ bicrystal substrates are used as templates to grow BiFeO₃ thin films with grain boundaries. Results of aberration-corrected scanning transmission electron microscopy (STEM) and piezoresponse force microscopy (PFM) suggest that 10°, 22.6° and 36.8° BiFeO₃ grain boundaries exhibit head-to-head polarization configurations. We characterize the atomic structure of these charged grain boundaries and find their width to be as narrow as ~1 nm. The polarization vectors on both sides of grain boundaries suggest unsuppressed polarization near the charged interfaces, indicating the polarization charges are likely to be well screened by mobile charges at grain boundaries. These results validate our strategy and provide a feasible way to obtain tunable charged interfaces in multiferroics via defects engineering for applications in nanoelectronics.

2. Experimental

2.1. Film growth

BiFeO₃ thin films were grown via pulsed laser deposition on 10°, 22.6°, and 36.8° SrTiO₃ bicrystals. SrTiO₃ bicrystals with [001] symmetric tilt grain boundaries were purchased commercially (Shinkosha Co. Ltd.). The orientation relationship of two single crystals is shown in Fig. S1 (online). The tilt angle can be defined as the angle between [100] direction of neighboring SrTiO₃ single crystals with [001] as the rotation axis. The temperature and gaseous environment during growth were fixed at 650 °C and 100 mTorr (1 Torr = 133.3 Pa) O₂ respectively. The laser (KrF, $\lambda = 248$ nm) energy density was 1.5 J cm⁻² at the target surface and the repetition rate was 10 Hz for BiFeO₃. After the growth, the samples were cooled down to room temperature at 10 °C min⁻¹ in 760 Torr oxygen ambient. The sample thickness was controlled by the growth time.

2.2. Samples preparation and STEM characterization

TEM samples were prepared by conventional mechanical polishing and subsequent argon ion milling in a Precision Ion Polishing System 691 (Gatan). The procedure for ion milling consisted of two steps. During the first stage, the guns were operated at 4 keV and at angles of 6°. During the second stage, the guns were operated at 1 keV for 5 min and at angles of 3°, and lowered further to 0.1 keV for 2 min for final surface cleaning. High-angle annular dark-field (HAADF) images and energy-dispersive X-ray spectroscopy (EDS) images in this work were obtained using probe Cs-corrected FEI Titan 60–300 (Titan Themis G2 in Electron Microscopy Laboratory of Peking University) operated at 300 kV. Atom positions were determined by simultaneously fitting two-dimensional Gaussian peaks to a perovskite unit cell using a home-developed code running in MATLAB. Polar displacements of the Fe cations were measured relative to the center of the surrounding Bi cations in HAADF images.

2.3. PFM test

PFM was performed on a commercial scanning probe microscope system (Asylum Research 3D) using commercial Pt/Ir-coated Si tips (Nanosensors) and Pt-coated Si tips (MikroMasch) at room temperature under ambient conditions. The PFM signal

was collected at the contact resonance frequency with an AC tip bias of 2 V.

2.4. X-ray diffraction (XRD) test

XRD measurements were carried out with a high-resolution diffractometer (Smartlab, Rigaku) using monochromatic Cu K_{α1} radiation ($\lambda = 1.5406$ Å).

3. Results and discussion

50-nm-thick BiFeO₃ thin films were deposited on SrTiO₃ bicrystal substrates. At room temperature, BiFeO₃ with the rhombohedral R3c structure is characterized by two perovskite unit cells connected along their body diagonal [30,31]. All Miller indices of BiFeO₃ in this study are based on the pseudocubic lattice. The spontaneous polarization is along the [111]_{pc} axis (where pc denotes pseudocubic indices) [32–34]. The tilt angle β of grain boundaries is tunable as illustrated by the schematic in Fig. 1a. Technically, BiFeO₃ could have eight possible polarization orientations in each grain. Due to the epitaxial relationship between films and substrates, grain boundaries in BiFeO₃ are expected to vary depending on grain boundaries of the underlying SrTiO₃. Fig. 1b depicts three XRD patterns corresponding to the epitaxial BiFeO₃ thin films on 10°, 22.6° and 36.8° SrTiO₃ bicrystals respectively, all of which clearly exhibit peaks corresponding to SrTiO₃ (001) and BiFeO₃ (001). The XRD scan in Fig. 1b indicates a high-quality epitaxial single-crystalline nature of BiFeO₃ thin films.

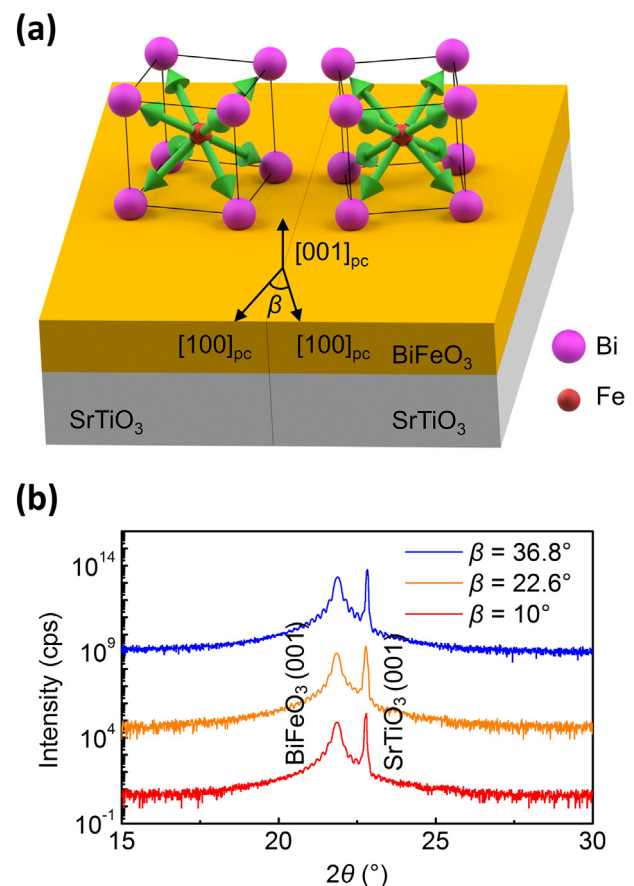


Fig. 1. (Color online) BiFeO₃ bicrystal thin film. (a) Schematic diagram of epitaxial BiFeO₃ thin films grown on SrTiO₃ bicrystal substrates. BiFeO₃ have eight possible polarization orientations. (b) XRD profiles of BiFeO₃/SrTiO₃ heterostructures revealing the highly crystalline quality of BiFeO₃ thin films.

To determine their domain structure, 10° , 22.6° and 36.8° BiFeO₃ grain boundaries were subjected to PFM analysis. Topographic and out-of-plane PFM measurements of grain boundaries revealed a small roughness (less than 6 nm) and uniform out-of-plane polarization (Fig. S2 online). Fig. 2a–c show the in-plane measurements near grain boundaries while Fig. 2d–f depict similar measurements in the same areas, albeit in the perpendicular scan directions. We also characterized the polarization orientation at BiFeO₃/SrTiO₃ interfaces (Fig. S3 online). The polarization orientation can be clearly determined by the contrast which suggests the head-to-head polarization configuration at grain boundaries. Two uniform contrast regions appear in the vicinity of ~ 400 nm from each grain boundary, evidencing while near the grain boundaries a monodomain structure exists. Sharp changes in contrast at the grain boundaries resemble those of the domain wall in adjacent BiFeO₃ thin films, but the limited resolution of PFM precludes evaluation of their width. The schematics in Fig. 2g–i unambiguously illustrate the polarization configuration at grain boundaries which retain their head-to-head polarization configuration regardless of the grain boundary angle. Moreover, increasing the films to 100 nm in thickness did not evoke a change to the head-to-head polarization configuration of the 10° , 22.6° and 36.8° grain boundaries (Fig. S4 online). In other words, the head-to-head polarization configuration is energetically favorable at these BiFeO₃ grain boundaries, which is likely because the positive bound charges can be more effectively screened by negative free carriers in BiFeO₃

[35,36]. Bismuth-based ferroelectric oxide films such as BiFeO₃ prepared by pulsed laser deposition (PLD) have been reported as n-type semiconductors [36–38], suggesting the negative charges (electrons and negatively charged point defects) in BiFeO₃ films could be accumulated at defects such as grain boundaries to screen the positive polarization bound charges. Besides, grain boundaries in oxides usually prefer to be non-stoichiometric which can lead to charge accumulation at these defects [39]. For example, Ti enrichment and deficiency has been reported at different SrTiO₃ grain boundaries [40,41], and oxygen vacancy was also detected at yttria-stabilized zirconia grain boundaries [42]. In our cases, the quantitatively elemental analysis of BiFeO₃ grain boundaries by EDS indicates the slight deficiency of Bi³⁺ and Fe³⁺ at grain boundaries (Fig. S5 online). Thus, the relative enrichment of oxygen can provide negative charges to screen the positive polarization bound charges at grain boundaries, which stabilizes the head-to-head polarization configurations.

To investigate the structure of charged grain boundaries at atomic scale, 10° , 22.6° and 36.8° grain boundaries were characterized by aberration-corrected STEM. The HAADF image in Fig. 3a shows the atomic structure of the 10° grain boundary. From this Z-contrast image [43], it is possible to distinguish the columns comprised of Bi atoms and Fe atoms, respectively. The corresponding fast Fourier transform (FFT) image confirms a tilt angle of 10° in BiFeO₃ grain boundary (Fig. S6 online). The width of the 10° grain boundary is about 2 unit cells (~ 1 nm). The atomic structures of the

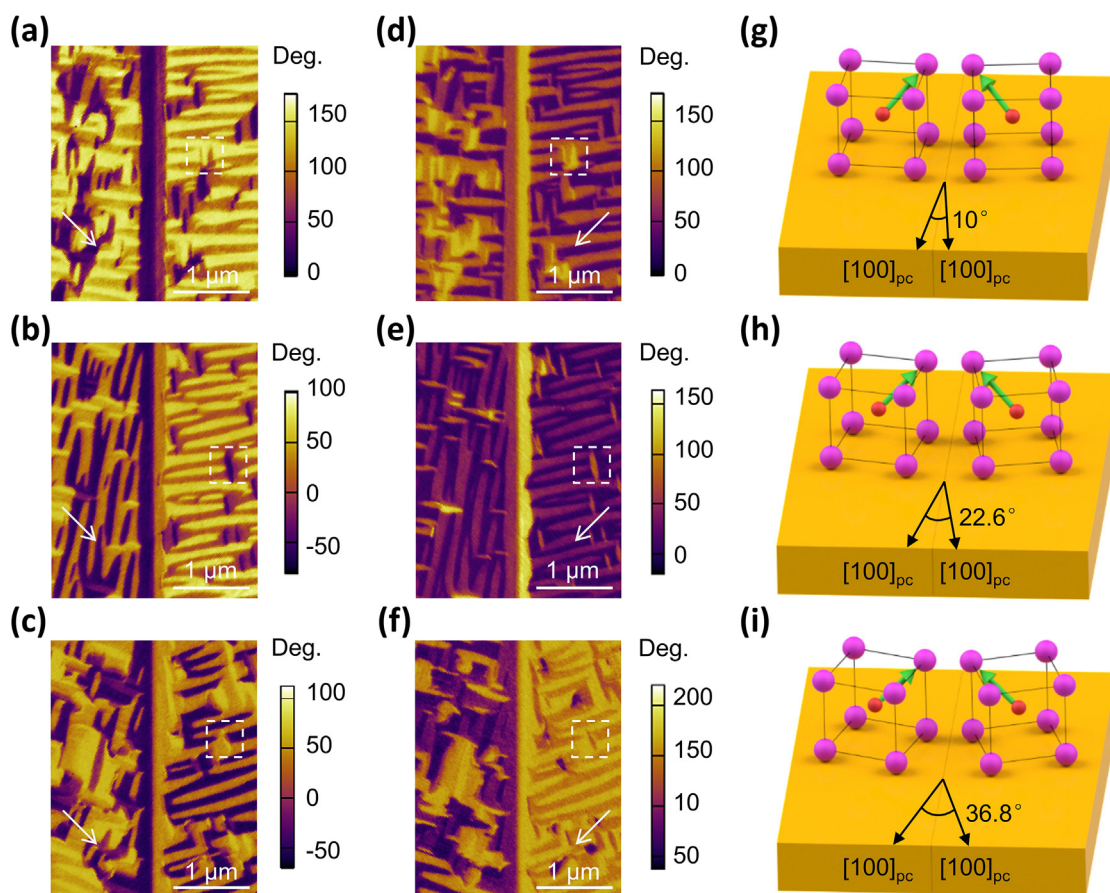


Fig. 2. (Color online) Domain structure of BiFeO₃ grain boundaries. (a–c) In-plane PFM measurements for 10° , 22.6° and 36.8° BiFeO₃ bicrystals thin films. Arrows indicate scan directions. (d–f) PFM measurements for the same areas of the 10° , 22.6° and 36.8° BiFeO₃ bicrystals respectively, albeit in the scan directions perpendicular to those in (a–c). Dashed rectangles denote the same area. Arrows indicate scan directions. (g–i) Schematic diagrams showing polarization configurations near grain boundaries. The green arrows show polarization of BiFeO₃ towards the grain boundary.

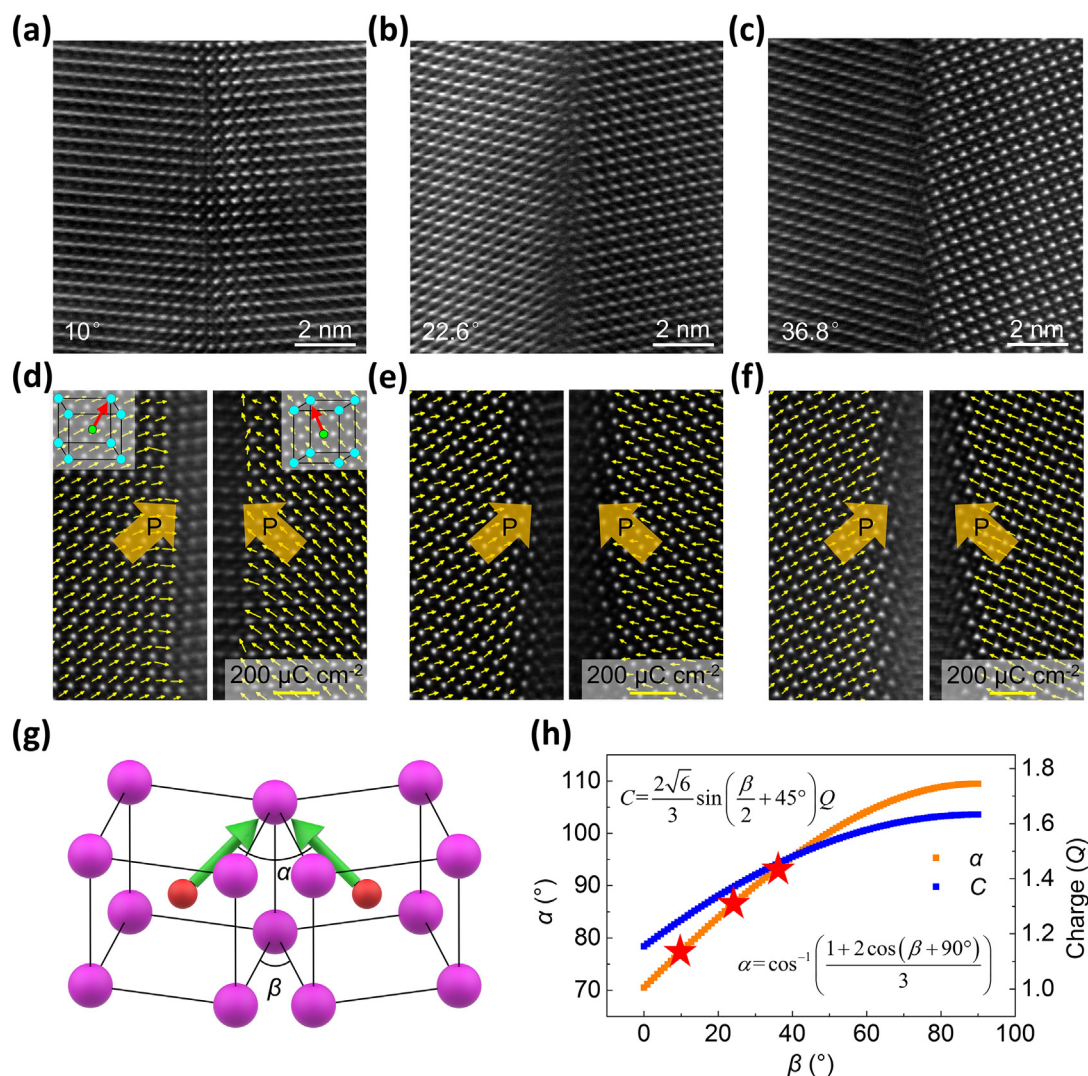


Fig. 3. (Color online) Atomic structure of BiFeO₃ grain boundaries. Atomic-resolution HAADF images of (a) 10°, (b) 22.6° and (c) 36.8° BiFeO₃ grain boundaries. Atomic images overlaid with polarization vectors of (d) 10°, (e) 22.6° and (f) 36.8° BiFeO₃ grain boundaries. The length of arrows indicates the magnitude of the polarization with respect to the yellow scale bar. (g) Schematic diagram of the geometric relationship between grain boundary angle and polarization configuration, where β denotes relative crystal disorientation angle and α denotes angle of polarization orientations. (h) α and charges C at grain boundaries as a function of β. The three stars correspond to 10°, 22.6°, and 36.8° BiFeO₃ grain boundaries in this study. Q indicates the polarization of BiFeO₃ films.

22.6° and 36.8° grain boundaries are shown in Fig. 3b and c, respectively. Despite many efforts, obtaining perfect atomic structure on both sides of a BiFeO₃ grain boundary simultaneously has remained challenging. Zone axes of two grains of BiFeO₃ are not consistent, making it difficult to perfectly observe the atomic structure of both grains at the same time. This may be rooted in the distorted structure of the combined rhombohedral BiFeO₃ bicrystals without the constraint from the SrTiO₃ substrate in plan-view TEM samples [44].

To further elucidate how polarization occurs at the grain boundaries, atomic-resolution images for both sides of grain boundaries were obtained and analyzed separately. From these HAADF images, we can precisely determine the positions of Bi atom columns and Fe atom columns. The polarization vectors of unit cells near the grain boundaries were mapped according to the relative displacement between Fe atom columns and the center of four neighboring Bi atom columns [24]. Fig. 3d depicts the representative HAADF images of the 10° grain boundary overlaid with the corresponding spatial distribution of polarization vectors, where arrow angle and length indicate the orientation and magni-

fication, respectively, of the projected polarization in each unit cell. Conventional understanding suggests that the polarization should be greatly suppressed at the charged interface [22,25]. Nevertheless, the polarization vectors are uniform even near the grain boundary. Similar results were obtained for 22.6° and 36.8° grain boundaries shown in Fig. 3e and f. Fig. 3g shows a schematic representation of α and β (where α is the angle of polarization orientations at BiFeO₃ grain boundaries and β is the angle of grain boundaries). The geometric relationship between α and β is shown in Fig. S7 (online, arrows indicate directions of polarization). For simplicity, we consider BiFeO₃ a cubic structure. The geometric relationship between α and β can be expressed as

$$\alpha = \cos^{-1}\left(\frac{1 + 2\cos(\beta + 90^\circ)}{3}\right). \quad (1)$$

The 10°, 22.6° and 36.8° grain boundaries exhibit 77°, 86° and 94° head-to-head polarization configurations respectively, indicating that continuous tuning of the angle of charged interfaces can be achieved by adjusting the grain boundary angle of the SrTiO₃ bicrystal substrates. Fig. 3h plots this relationship. Therefore, the

polarization charge C at grain boundaries resulting from head-to-head polarization configurations can be expressed as a function of β which is shown in Fig. 3h. The discrete three points in plots represent the experimental measurements of 10° , 22.6° and 36.8° grain boundaries in this study. These plots can guide strategic design of grain boundaries with tunable polarization charges by manipulating the angle of SrTiO_3 bicrystal from 0° to 90° . This general and feasible method creates new avenues towards the development of innovative charged interfaces which are absent in regular multiferroics.

Identifying the atomic structure is critical for a comprehensive understanding of BiFeO_3 grain boundaries. Grain boundaries of some crystals such as SrTiO_3 have been characterized thoroughly with respect to their atomic structures and local electronic structures via advanced atomic-resolution imaging and electron energy loss spectroscopy [39,40,45]. In contrast, there exist few reports of the atomic structure of BiFeO_3 grain boundaries, especially by TEM methods, perhaps due to limitations of the thin-film growth technology and the low mechanical stability of BiFeO_3 [46–49]. After many careful attempts, we obtained the atomic structure reported in this study and demonstrated that the width of BiFeO_3 grain boundaries can be as narrow as ~ 1 nm.

The BiFeO_3 grain boundary in this study exhibits head-to-head polarization configuration and offers an alternative tool for fabricating tunable charged interfaces in ferroelectric thin films. The width of such grain boundary is as narrow as the as-grown 180° , 109° or 71° domain walls in BiFeO_3 thin films [33]. These kinds of charged interfaces possess anomalous polarization configurations compared with conventional 180° , 109° and 71° domain walls in BiFeO_3 thin films. They are also robust and therefore retain these polarization configurations despite changes in film thicknesses and external stimuli. Since the maximum grain boundary angle of tilt SrTiO_3 bicrystals is 90° (schematically shown in Fig. S7 online), adjusting the angle of SrTiO_3 bicrystal from 0° to 90° enables tunable polarization configurations between 71° and 109° , indicating that precise design of the type of such charged interfaces is possible. Such charged grain boundaries are expected to produce many novel properties such as conductivity [18,50], magnetoelectric properties [8] and photoconductivity [9]. Undoubtedly, further research will lead to the discovery of innovative approaches to apply these promising charged grain boundaries and achieve their practical application.

4. Conclusion

In summary, we have presented a general and viable method to create tunable grain boundaries with head-to-head polarization configurations in BiFeO_3 thin films. We also demonstrated the atomic structure for 10° , 22.6° , and 36.8° BiFeO_3 charged grain boundaries whose single head-to-head polarization configuration and adjacent monodomain structure indicate that charged grain boundaries are uniform and can therefore be readily designed and controlled. Direct observation of the atomic structure of charged grain boundaries via aberration-corrected STEM revealed the identical polarization on either side of the grain boundaries. In addition, the polarization configuration of the charged interfaces was demonstrated to be tunable from 71° to 109° by adjusting the angle of SrTiO_3 bicrystal to control interfacial charge density. Our strategy leverages grain boundary engineering for tunable charged interfaces in BiFeO_3 , although it may be extended to other types of ferroelectric materials with perovskite structure, such as PbTiO_3 and BaTiO_3 . The ability to controllably fabricate charged interfaces offers new routes towards the development of applications of multiferroic thin films in nanoelectronics.

Conflict of interest

The authors declare that they have no conflict of interest.

Acknowledgments

This work at Peking University was supported by the National Basic Research Program of China (2016YFA0300804), the National Natural Science Foundation of China (51672007 and 11974023), Key Area R&D Program of Guangdong Province (2018B010109009), the Key R&D Program of Guangdong Province (2018B030327001), National Equipment Program of China (ZDYZ2015-1), and the “2011 Program” Peking-Tsinghua-IOP Collaborative Innovation Centre for Quantum Matter. This work at Tsinghua University was supported by the National Basic Research Program of China (2016YFA0301004), the National Natural Science Foundation of China (51872155, 52025024), and the Beijing Advanced Innovation Center for Future Chip (ICFC).

Author contributions

Mingqiang Li carried out TEM experiments, analyzed the data and wrote the manuscript under the direction of Peng Gao. Ruochen Shi, Ruixue Zhu, Xiaomei Li and Yang Cheng assisted the data analysis. Shuzhen Yang grew the samples and carried out PFM tests, and Linglong Li carried out conductive atomic force microscopy tests under the direction of Pu Yu. Peng Gao directed the project. The manuscript was written through contributions of all authors. All authors have given approval to the final version of the manuscript.

Appendix A. Supplementary materials

Supplementary materials to this article can be found online at <https://doi.org/10.1016/j.scib.2020.12.032>.

References

- [1] Seidel J. Topological structures in ferroic materials. Switzerland: Springer International Publishing 2016.
- [2] Thiel S, Hammerl G, Schmehl A, et al. Tunable quasi-two-dimensional electron gases in oxide heterostructures. *Science* 2006;313:1942–5.
- [3] Tian G, Yang W, Song X, et al. Manipulation of conductive domain walls in confined ferroelectric nanoislands. *Adv Funct Mater* 2019;29:1807276.
- [4] Gozar A, Logvenov G, Kourkoutis LF, et al. High-temperature interface superconductivity between metallic and insulating copper oxides. *Nature* 2008;455:782–5.
- [5] Herranz G, Basletić M, Bibes M, et al. High mobility in $\text{LaAlO}_3/\text{SrTiO}_3$ heterostructures: origin, dimensionality, and perspectives. *Phys Rev Lett* 2007;98:216803.
- [6] Chakhalian J, Freeland JW, Srajer G, et al. Magnetism at the interface between ferromagnetic and superconducting oxides. *Nat Phys* 2006;2:244–8.
- [7] Gupta R, Chaudhary S, Kotnala RK. Interfacial charge induced magnetoelectric coupling at $\text{BiFeO}_3/\text{BaTiO}_3$ bilayer interface. *ACS Appl Mater Interfaces* 2015;7:8472–9.
- [8] Kumari S, Ortega N, Kumar A, et al. Dielectric anomalies due to grain boundary conduction in chemically substituted BiFeO_3 . *J Appl Phys* 2015;117:114102.
- [9] Nandy S, Mocherla PSV, Sudakar C. Photoconductivity induced by nanoparticle segregated grain-boundary in spark plasma sintered BiFeO_3 . *J Appl Phys* 2017;121:203102.
- [10] Liu S, Zheng F, Koocher NZ, et al. Ferroelectric domain wall induced band gap reduction and charge separation in organometal halide perovskites. *J Phys Chem Lett* 2015;6:693–9.
- [11] Hwang HY, Iwasa Y, Kawasaki M, et al. Emergent phenomena at oxide interfaces. *Nat Mater* 2012;11:103–13.
- [12] Catalan G, Seidel J, Ramesh R, et al. Domain wall nanoelectronics. *Rev Mod Phys* 2012;84:119–56.
- [13] Seidel J. Domain walls as nanoscale functional elements. *J Phys Chem Lett* 2012;3:2905–9.
- [14] Niranjan MK, Wang Y, Jaswal SS, et al. Prediction of a switchable two-dimensional electron gas at ferroelectric oxide interfaces. *Phys Rev Lett* 2009;103:016804.
- [15] Liu Y, Zhu Y-L, Tang Y-L, et al. Local enhancement of polarization at $\text{PbTiO}_3/\text{BiFeO}_3$ interfaces mediated by charge transfer. *Nano Lett* 2017;17:3619–28.

- [16] Ohtomo A, Hwang HY. A high-mobility electron gas at the LaAlO₃/SrTiO₃ heterointerface. *Nature* 2004;427:423–6.
- [17] Fujisawa H, Seto S, Nakashima S, et al. Introduction of an artificial domain wall into BiFeO₃ thin film using SrTiO₃ bicrystal substrate. *Jpn J Appl Phys* 2015;54:10NA06.
- [18] Rodriguez BJ, Chu YH, Ramesh R, et al. Ferroelectric domain wall pinning at a bicrystal grain boundary in bismuth ferrite. *Appl Phys Lett* 2008;93:142901.
- [19] Marincel DM, Zhang H, Kumar A, et al. Influence of a single grain boundary on domain wall motion in ferroelectrics. *Adv Funct Mater* 2014;24:1409–17.
- [20] Gureev MY, Tagantsev AK, Setter N. Head-to-head and tail-to-tail 180° domain walls in an isolated ferroelectric. *Phys Rev B* 2011;83:184104.
- [21] Feigl L, Sluka T, McGilly LJ, et al. Controlled creation and displacement of charged domain walls in ferroelectric thin films. *Sci Rep* 2016;6:31323.
- [22] Tang YL, Zhu YL, Wang YJ, et al. Atomic-scale mapping of dipole frustration at 90 degrees charged domain walls in ferroelectric PbTiO₃ films. *Sci Rep* 2014;4:4115.
- [23] Li M, Cheng X, Li N, et al. Atomic-scale mechanism of internal structural relaxation screening at polar interfaces. *Phys Rev B* 2018;97:180103.
- [24] Li L, Gao P, Nelson CT, et al. Atomic scale structure changes induced by charged domain walls in ferroelectric materials. *Nano Lett* 2013;13:5218–23.
- [25] Jia C-L, Mi S-B, Urban K, et al. Atomic-scale study of electric dipoles near charged and uncharged domain walls in ferroelectric films. *Nat Mater* 2008;7:57–61.
- [26] Eliseev EA, Morozovska AN, Svechnikov G, et al. Static conductivity of charged domain walls in uniaxial ferroelectric semiconductors. *Phys Rev B* 2011;83:235313.
- [27] Sturman B, Podivilov E, Stepanov M, et al. Quantum properties of charged ferroelectric domain walls. *Phys Rev B* 2015;92:214112.
- [28] Qi Y, Chen Z, Huang C, et al. Coexistence of ferroelectric vortex domains and charged domain walls in epitaxial BiFeO₃ film on (110)₀ GdScO₃ substrate. *J Appl Phys* 2012;111:104117.
- [29] Han M-G, Marshall MSJ, Wu L, et al. Interface-induced nonswitchable domains in ferroelectric thin films. *Nat Commun* 2014;5:4693.
- [30] Ederer C, Spaldin NA. Effect of epitaxial strain on the spontaneous polarization of thin film ferroelectrics. *Phys Rev Lett* 2005;95:257601.
- [31] Zavaliche F, Yang SY, Zhao T, et al. Multiferroic BiFeO₃ films: domain structure and polarization dynamics. *Phase Transit* 2006;79:991–1017.
- [32] Cruz MP, Chu YH, Zhang JX, et al. Strain control of domain-wall stability in epitaxial BiFeO₃ (110) films. *Phys Rev Lett* 2007;99:217601.
- [33] Wang Y, Nelson C, Melville A, et al. BiFeO₃ domain wall energies and structures: a combined experimental and density functional theory + U study. *Phys Rev Lett* 2013;110:267601.
- [34] Rossell MD, Erni R, Prange MP, et al. Atomic structure of highly strained BiFeO₃ thin films. *Phys Rev Lett* 2012;108:047601.
- [35] Seidel J, Martin LW, He Q, et al. Conduction at domain walls in oxide multiferroics. *Nat Mater* 2009;8:229–34.
- [36] Liu Z, Yan F, Hintzen H. The application of bismuth-based oxides in organic-inorganic hybrid photovoltaic devices. *J Am Ceram Soc* 2012;95:1944–8.
- [37] You T, Shuai Y, Luo W, et al. Exploiting memristive BiFeO₃ bilayer structures for compact sequential logics. *Adv Funct Mater* 2014;24:3357–65.
- [38] Farokhipoor S, Noheda B. Conduction through 71 degrees domain walls in BiFeO₃ thin films. *Phys Rev Lett* 2011;107:127601.
- [39] Gao P, Yang S, Ishikawa R, et al. Atomic-scale measurement of flexoelectric polarization at SrTiO₃ dislocations. *Phys Rev Lett* 2018;120:267601.
- [40] Takehara K, Sato Y, Tohei T, et al. Titanium enrichment and strontium depletion near edge dislocation in strontium titanate [001]//(110) low-angle tilt grain boundary. *J Mater Sci* 2014;49:3962–9.
- [41] Li X, Chen S, Li M, et al. Atomic origin of Ti-deficient dislocation in SrTiO₃ bicrystals and their electronic structures. *J Appl Phys* 2019;126:174106.
- [42] Feng B, Lugg NR, Kumamoto A, et al. Direct observation of oxygen vacancy distribution across yttria-stabilized zirconia grain boundaries. *ACS Nano* 2017;11:11376–82.
- [43] Pennycook SJ, Boatner LA. Chemically sensitive structure-imaging with a scanning transmission electron microscope. *Nature* 1988;336:565–7.
- [44] Chen ZH, Damodaran AR, Xu R, et al. Effect of “symmetry mismatch” on the domain structure of rhombohedral BiFeO₃ thin films. *Appl Phys Lett* 2014;104:182908.
- [45] Buban JP, Chi M, Masiel DJ, et al. Structural variability of edge dislocations in a SrTiO₃ low-angle [001] tilt grain boundary. *J Mater Res* 2009;24:2191–9.
- [46] Rodriguez BJ, Choudhury S, Chu Y, et al. Unraveling deterministic mesoscopic polarization switching mechanisms: spatially resolved studies of a tilt grain boundary in bismuth ferrite. *Adv Funct Mater* 2009;19:2053–63.
- [47] Zeches RJ, Rossell M, Zhang J, et al. A strain-driven morphotropic phase boundary in BiFeO₃. *Science* 2009;326:977–80.

- [48] Zhang J, Ke X, Gou G, et al. A nanoscale shape memory oxide. *Nat Commun* 2013;4:3768.
- [49] Yu P, Luo W, Yi D, et al. Interface control of bulk ferroelectric polarization. *Proc Natl Acad Sci USA* 2012;109:9710–5.
- [50] Lin Ye, Fang S, Su D, et al. Enhancing grain boundary ionic conductivity in mixed ionic–electronic conductors. *Nat Commun* 2015;6:7824.



Mingqiang Li is currently a Ph.D. candidate in Department of Materials Science and Engineering, University of Toronto. He received his M.Sc. degree in Condensed Matter Physics from Peking University in 2020, and B.E. degree from Zhengzhou University in 2016. His research interest focuses on the structure-property relationships of ferroelectrics and nanomaterials by using *in situ* transmission electron microscopy.



Shuzhen Yang received his Ph.D. degree from Department of Physics, Tsinghua University in 2019. He mainly studied the interfacial properties of multiferroic materials, such as BiFeO₃, and used piezoelectric force microscopes to study the properties of ferroelectric domain walls and domains.



Pu Yu is a professor at Department of Physics, Tsinghua University. He received his Ph.D. degree in Physics from University of California at Berkeley in 2011. After one-year postdoc stay at RIKEN, he joined the faculty of Tsinghua University as an assistant professor in 2012, and was promoted to associate professor in 2017 and then professor in 2018. His current research interest lies in understanding and designing novel electronic states within complex oxide heterostructures.



Peng Gao is an assistant professor in School of Physics, Peking University. He received his Ph.D. degree in Condensed Matter Physics from the Institute of Physics, Chinese Academy of Sciences in 2010. He was a post-doctor in University of Michigan (2010–2013), research associate in Brookhaven National Lab (2013–2014), research fellow and Japan Society for the Promotion of Science (JSPS) foreign fellow in University of Tokyo (2014–2015). He joined Peking University in 2015. His main research interest is probing interfaces in quantum materials via electron scattering.